JKAU: Eng. Sci., vol. 8, pp. 21-35 (1416 A.H./1996 A.D.)

Circuit Interruption Phenomena in Three-Phase Multiconductor Transmission Systems

S.E.T. MOHAMED, A.U.M. ABDUL-AZIZ and A.H. MUFTI
Electrical and Computer Engineering Department,
Faculty of Engineering, King Abdulaziz University,
Jeddah, Saudi Arabia

ABSTRACT. With a rising trend for transmission system voltages in the EHV and UHV ranges and a consequent increase in insulation costs of these networks together with their associated equipment, the need for rigorous system analysis for the sake of optimal design considerations is realized. This paper highlights the significance of fairly accurate analysis of interruption phenomena in three-phase multiconductor transmission systems as an essential prerequisite for the optimal design and operational requirements of interruption equipment. A mathematical algorithm has been developed in the paper to simulate very accurately the transient wave-front of fault current following fault inception. The development is then implemented to compute waveforms of recovery transient voltages at circuit breaker location in the crucial microseconds succeeding contact separation. In the paper distributed parameter as well as frequency dependance effects are being considered. Furthermore the influence of source effects on the recovery transient initial rate of rise and on its maximum values are adequately highlighted.

1. Introduction

The analysis of circuit interruption phenomena in three-phase multiconductor transmission systems is of prime importance for planning, design and operation strategies of these networks. This is particularly emphasized as transmission voltages continue to increase in the EHV and UHV ranges in order to satisfy the ever increasing demand for electrical energy. With such high level operating voltages, continued efforts are being made to optimize laying down design specifications for system insulation coordination considering that insulation costs rise very rapidly with working system voltages[1].

The current paper considers a proposed technique for accurate assessment of circuit interruption of three-phase multiconductor transmission systems. This conforms with present-day trends which call for more rigorous analysis of these systems with a view to procure optimal design considerations[2-6]. The technique is based on the theory of natural modes[7-9] and the modified Fourier Transform methods for fast transient calculations[10,11]. Both the distributed nature and frequency dependance of system parameters have been accounted for.

The paper will demonstrate how, following fault inception, transient fault currents may be evaluated for short line faults of a 380 kV multiconductor line and also how the wave-fronts of such currents may be accurately reproduced around the zero cross-over point needed for simulation of the phenomena of circuit interruption. Furthermore, during the crucial microseconds following separation of circuit breaker contacts, the paper analyses the problem of the recovery voltage transient which is detrimental to the success of circuit interruption[12]. It shows how computer models may be built in order to evaluate the wave-front and peak value of such recovery transient[13] with a high degree of accuracy taking into consideration both line-side and source-side transient effects[14-18].

The paper concludes by presenting some computational results to validate the proposed technique for a number of operating system conditions.

2. Natural Modes Theory and Fourier Transform Methods

From the instant of fault inception to the time of circuit interruption, the transmission system undergoes a fast transient process. The accurate solution of this process has been carried out by application of the theory of natural modes and Fourier Transform methods[4,9]. Special algorithms have been developed by these techniques to suit the analysis of transient fault problem and circuit interruption in multiconductor transmission systems.

In the the following sections a brief summary of basic relationships for the theory of natural modes and Fourier Transform methods is presented. In addition and following the occurance of a fault on the line, the transform of the resultant fault current is evaluated.

2.1 Theory of Natural Modes

The basic line equations for a multiconductor transmission line are given by

$$\frac{d^2 V}{dX^2} = [\,Z\,]\,[\,Y\,]\,[\,V\,] \tag{1}$$

$$\frac{d^2 I}{dX^2} = [\,Y\,]\,[\,Z\,]\,[\,I\,] \tag{2}$$

where $[\,V\,]$ and $[\,I\,]$ are the conductor's voltage and current vectors, while $[\,Z\,]$ and $[\,Y\,]$ are the multiconductor line impedance and admittance matrices.

The complexity in the solution of Equations (1) and (2) has been resolved by the theory of natural modes[7]. A 2-port network representation has been developed for the solution of the steady-state problem. The voltage and current relationships for the input and output terminals are given by the following nodal admittance matrix equation

$$\begin{bmatrix} I_1 \\ I_2 \end{bmatrix} = \begin{bmatrix} A & -B \\ -B & A \end{bmatrix} \begin{bmatrix} V_1 \\ V_2 \end{bmatrix} \tag{3}$$

where

$$[\,A\,] = [\,Y_0\,]\,[\,\coth \psi l\,]$$

$$[\,B\,] = [\,Y_0\,]\,[\,\operatorname{cosech} \psi l\,]$$

$$l = \text{line length in m.}$$

$[\,A\,]$ and $[\,B\,]$ are symmetric matrices. $[\,Y_0\,]$ is the line's surge admittance matrix. ψ is a matrix function given by $\psi = Q\,\gamma\,Q^{-1}$, where Q is the eigenvector voltage transformation matrix and $[\,\gamma\,]$ is line's propagation constant matrix.

Equation (3) yields the steady-state solution of the three-phase transmission system problem. It is necessary to combine this equation with the Fourier Transform method in order to obtain solution of the transient problem. The well established Modified Fourier Transform technique has demonstrated its success in dealing with fast transients problems in transmission systems.

2.2 Modified Fourier Transform

The Fourier Transform and its inverse are given by

$$F(\omega) = \int_{-\infty}^{+\infty} F(t)\, e^{-j\omega t}\, dt \tag{4}$$

$$F(t) = \frac{1}{2\pi} \int_{-\infty}^{+\infty} F(\omega)\, e^{j\omega t}\, d\omega \tag{5}$$

Day, *et al.*[10] developed a modified version for the Fourier Transform and its inverse in order to overcome some of the difficulties met in the direct application of Equations (4) and (5). The modified version is given

$$F(\omega - ja) = \int_0^{\Omega} F(t)\, e^{-at}\, e^{-j\omega t}\, dt \tag{6}$$

$$F(t) = \frac{e^{at}}{\pi} \int_0^{T} F(\omega - ja)\, e^{j\omega t}\, \sigma\, d\omega \tag{7}$$

where

Ω = an upper trancation frequency
a = a shift constant
σ = $\sin(\pi\omega / T) / (\pi\omega / T)$, a smoothing factor
T = observation time of transient

ω = angular frequency variable
T = time variable

For computational purposes a number of half range expansions may be used for evaluating the transient response, such as

$$F(t) = \text{Real}\ \frac{e^{at}}{\pi} \int_0^T F(\omega - ja)\ e^{j\omega t} \cdot \sigma \cdot d\omega \tag{8}$$

If odd harmonics are selected with step length twice the value of fundamental frequency ($2\ \omega_0$), then Equation (8) becomes

$$F(t) = \frac{e^{at}}{2\pi}\ 2\omega_0\ \text{Real} \sum_{n=1}^{N-1} F(\omega - ja)\ e^{j\omega t} \cdot \sigma \tag{9}$$

Where

$2N$ = total number of harmonics chosen for the evaluation of the frequency response
ω = $(2n-1)\omega_0$
σ = $\dfrac{\sin[\pi(2n-1)/(2N-1)]}{[\pi(2n-1)/(2N-1)]}$, known as sigma factor.
ω_0 = π / T_0
T_0 = observation period

2.3 Transform of Fault Current

A cancellation voltage is applied at the fault location, Fig. 1(a). The system data is given in the Appendix II. Use is made of Superposition and Norton's theorem to simulate the fault condition at the fault point taking into consideration sound phase and faulty phase cases. Figure 1(b) shows the equivalent 2-port network. Terminal 1 is the source end while terminal 2 is the faulted end. Y_s and Y_f are suitable source and fault admittance matrices. Based on Fig. 1b the following relations are true.

$$\begin{bmatrix} I_1 \\ I_2 \end{bmatrix} = \begin{bmatrix} A + Y_s & -B \\ -B & A + Y_f \end{bmatrix} \begin{bmatrix} V_1 \\ V_2 \end{bmatrix} \tag{10}$$

As terminal 2 is faulted, $[\ I_1\ ]^t = [\ 0\ 0\ 0\ ]$ and $[\ I_2\ ]^t = [\ Y_f \cdot E_s\ 0\ 0\ ]$, where E_s is the

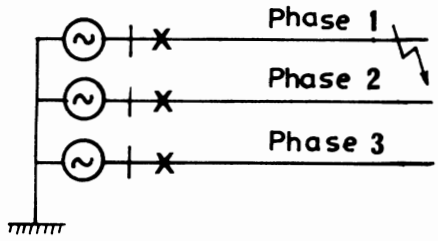

FIG. 1(a). Single-phase-to ground fault.

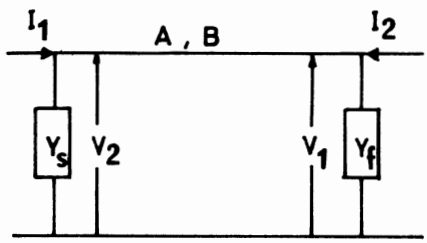

FIG. 1(b). Two-port equivalent.

steady-state voltage existing in phase prior to fault inception, and t denotes transpose of vector.

Consequently solving for frequency domain voltage and fault current I_f at circuit breaker location yields

$$0 = (A + Y_s) V_1 - BV_2 \tag{11}$$

$$Y_f E_s = -BV_1 + (A + Y_f) V_2 \tag{12}$$

giving finally

$$V_1 = [(A + Y_f) B^{-1} (A + Y_s) - B]^{-1} Y_f E_s \tag{13}$$

$$I_f = Y_s V_1 \tag{14}$$

Equations (13) and (14) represent the Fourier Transform of bus voltage and fault current. The time domain solutions for Equations (13) and (14) are obtained by the inverse transform of these equations.

3. Analysis Models for Circuit Interruption

The recovery transient voltage calculations are based on three distinct mathematical models. One basic model describes the analysis of fault current following fault inception. For this solution of the line's steady-state equations are derived and the Modified Fourier Transform technique is used to obtain the system fast response due to fault occurance. Of particular interest during this period are the waveforms of transient fault current and voltage at the circuit breaker location. Another model is required to define fairly accurately the wave-front of transient fault current around the zero cross-over point where circuit interruption is expected to take place.

Furthermore a recovery transient model is needed to describe the recovery transient phenomena in three phase systems. Such models will now be briefly explained.

3.1 Fault Inception Model

The well known principle of cancellation is employed. If a $(1 - \phi - G)$ fault develops on phase 1, then at the instant of fault inception, the overall fault current is obtained by superimposing the steady-state component prior to fault occurance with the resulting transient component. The resultant current is the bus fault current at the circuit breaker location.

3.2 Fault Current Synthesis Model

Following fault inception and depending on the speed of protective system, the transient fault current computation is stopped around a specified current zero cross-over where circuit interruption is contemplated. The duty of the current synthesis model is to determine fairly accurately the wavefront of the transient fault current around the zero cross-over point at which the circuit breaker contacts begin to separate. It is worthy of note that the transient fault current computation progresses for a short time interval after current zero, which period represents the time of interest for observation of the recovery voltage transient.

Figures 2(a) and 2(b) show a hypothetical waveform of fault current transient with an indentical current to be injected at the breaker terminal for cancellation purposes. The regular time interval for computation of the transient response is Δt whereas $k \Delta t$ is a fraction of Δt indicating the time of zero cross-over. On the basis of linear segments of transient fault current intervals Δt and $k \Delta t$, the precise time for circuit interruption T is obtained from

$$T = n \Delta t - \frac{f_n \cdot \Delta t}{f_n - f_{n-1}} \tag{15}$$

Also

$$k \Delta t = \frac{f_n \cdot \Delta t}{f_n - f_{n-1}} \tag{16}$$

where, f_n , f_{n-1} are the system response at the nth and $(n-1)$th time interval. n being the interval count.

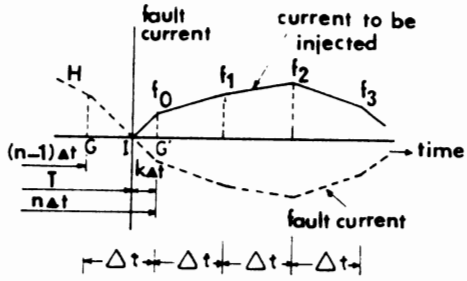

FIG. 2(a). Synthesis of recovery transient current.

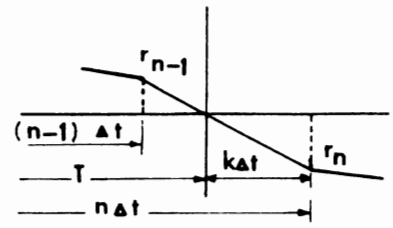

FIG. 2(b). Zero-crossing time step.

The mathematical formulation of the Fourier Transform of the cancellation current to act as a stimulus at the circuit breaker terminal is now obtained from the discrete values of fault current response.

$$F(\omega) = \frac{1}{j\omega}\left[f_0 \left(1 - \frac{1}{j\omega \Delta t}\right) + \frac{f_1}{j\omega \Delta t} + \left[\frac{f_{N-1}}{j\omega \Delta t} - f_N \left(1 + \frac{1}{j\omega \Delta t}\right)\right] e^{-j\omega N \Delta t} \right.$$

$$\left. + \left(\frac{1}{j\omega \Delta t}\right) \sum_{r=1}^{N-1} \left[(f_{r+1} - 2f_r + f_{r-1})\, e^{-j\omega_r \Delta t} \right] \right] e^{-j\omega k \Delta t}$$

$$+ \frac{1}{j\omega}\left[\frac{f_0}{j\omega k \Delta t} - f_0 \left(1 + \frac{1}{j\omega k \Delta t}\right) e^{-j\omega k \Delta t} \right] \tag{17}$$

where,

ω = $(2n - 1)\ \omega_n$
ν_n = π / T_x
T_x = observation time for recovery transient period.
ΔT = time step for fault current calculation.
N = number of discrete values of fault current.

3.3 Recovery Voltage Transient Model

Figure 3(a) shows a faulted three-phase transmission line with a last breaker pole-to-clear. The equivalent circuit is shown in Fig. 3(b). Using nodal equation with a fault current stimulus I_f, the model for recovery voltage is given as follows

$$\begin{bmatrix} I_f \\ 0 \end{bmatrix} = \begin{bmatrix} A + Y_S & -B \\ -B & A + Y_f \end{bmatrix} \begin{bmatrix} V_{SL} \\ V_r \end{bmatrix} \tag{18}$$

where,

V_{SL} = line-side recovery voltage transform.
V_r = fault point voltage transform.
I_f = injected fault current transform.
Y_f = terminal fault admittance matrix.
Y_s = terminal source admittance matrix.
A, B = line matrix constants.

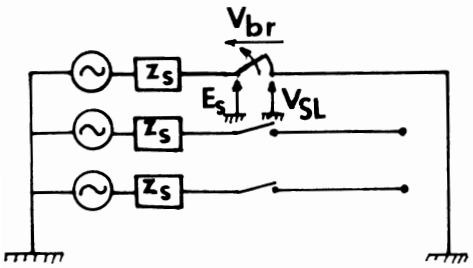

FIG. 3(a). Last pole-to-clear.

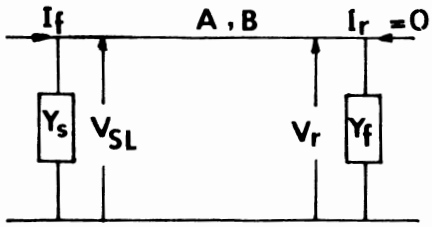

FIG. 3(b). Two-port-equivalent.

Solving (18) yields the recovery voltage transform

$$V_{SL} = [(A + Y_s) - B(A + Y_f)^{-1} B]^{-1} I_f \tag{19}$$

Solution of Equation (19) in the time domain gives the recovery voltage transient on the line side of the circuit breaker. To obtain the voltage across the circuit breaker (V_{BR}) this is given by the difference of steady-state voltage on the source side (E_S) and line side (V_{SL}) of the breaker, namely

$$V_{BR} = E_S - V_{SL} \tag{20}$$

The recovery voltage V_{BR} given in Equation (20) ignores the effect of the circuit on

the source side voltage (V_{SS}). For extreme accuracy, however, the source side transient voltage, or supply transient should be taken into consideration. This is particularly important as the rate of rise and peak value of the breaker recovery voltage may be significantly influenced by the component of supply transient. Sources are usually fed from transformers, and in practice lumped capacitance due to CT's and VT's may exist at the breaker terminals and consequently their influence must be considered in the simulation process.

3.4 Source-Side Voltage Synthesis

To take into consideration the influence of the source side transient component, the Fourier Transform of the source-side voltage wave is carried out. Figure 3(c) shows typical discrete time domain values for the computed source-side transient voltage obtained around the instant of circuit interruption T. The Fourier Transform F (ω) for this component is given by

$$F(\omega) = \frac{1}{j\omega}\left\{ f_0\left(1 - \frac{1}{j\omega\Delta t}\right) + \frac{f_1}{j\omega\Delta t} + \left[\frac{f_{N-1}}{j\omega\Delta t} - f_N\left(1 + \frac{1}{j\omega\Delta t}\right)\right] e^{-j\omega N\Delta t} \right.$$
$$\left. + \frac{1}{j\omega\Delta t}\sum\left[\left(f_{r+1} - 2f_r + f_{r-1}\right) e^{-j\omega_r\Delta t}\right] \right\} e^{-j\omega k\Delta t}$$
$$+ \frac{1}{j\omega}\left\{ f_0\,\frac{(\Delta t - k\Delta t)}{\Delta t} + f_{-1}\,\frac{k\Delta t}{\Delta t} \right.$$
$$\left. + \frac{1}{j\omega k\Delta t}\left[f_0 - \left[f_0\,\frac{(\Delta t - k\Delta t)}{\Delta t} + f_{-1}\,\frac{k\Delta t}{\Delta t}\right]\right]\right. \tag{21}$$

Setting $V_{SS} = F(\omega)$ (22)

the recovery voltage transform across the breaker terminals may now be accurately obtained taking into account the effect of the source side transient. This is given by

$$V_{BR} = V_{SS} - V_{SL} \tag{23}$$

The inverse transform of Equation (23) then yields the solution for the recovery transient across the circuit breaker terminals. The computer program chart shown in Appendix 1 clarifies the procedure.

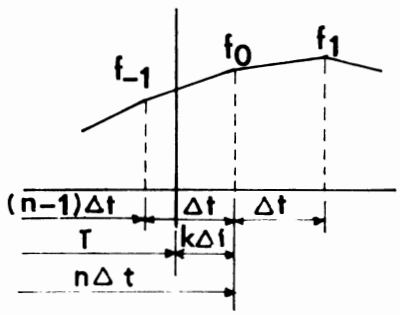

FIG. 3(c). Voltage synthesis.

4. Computational Results and Discussion

For investigation purposes a 20 km, 380 kv three-phase multiconductor line is considered with a single line-to-ground fault occuring at its far end of one phase as the voltage on that phase is passing through its maximum value. A variety of operating conditions have been considered to illustrate the principles presented in the paper with regard to circuit interruption in three-phase multiconductor transmission systems. (Line data are presented in Appendix II).

4.1 Infinite Bus-Bar Source

Figure 4(a) shows the transient fault current waveform for $1 - \phi - G$ fault on phase 1. Phases 2 and 3 are unfaulted and the system is initially unloaded. The faulted phase current is clearly distorted during the initial stages of fault occurance due to successive reflection between source and fault terminations. Phases 2 and 3 transient currents are almost negligible. These minor components are due to mutual coupling between sound and healthy phases. Figure 4(b) shows the voltage waveforms at the source termination, and as expected due to infinite bus source these waveforms are pure simnusoidal waves.

Circuit interruption has been carried out at the second zero cross-over with a last pole to clear. Figure 4(c) shows source-side and line-side voltage following separation of breaker contacts. It also shows the recovery voltage transient across the circuit breaker. As expected, the line-side transient waveform is characterised by the line's natural oscillations. These oscillations are damped out due to system losses in about 800 μsec. The recovery voltage across the breaker rises steeply at an initial rate of 2.2 kv/μsec to a peak value of 1.5 p.u. voltage then decays to the steady-state value of the infinite bus source. The source-side voltage is a pure cosine wave and this is clearly reproduced over the stated observation time by using the proposed synthesis algorithm for voltage waveform.

Figure 4(d) shows similar results for the above network but with a longer observation time of 4000 μsec for the transient period. This longer observation period clearly indicates the damping effect of the voltage transients due to system losses. It is of in-

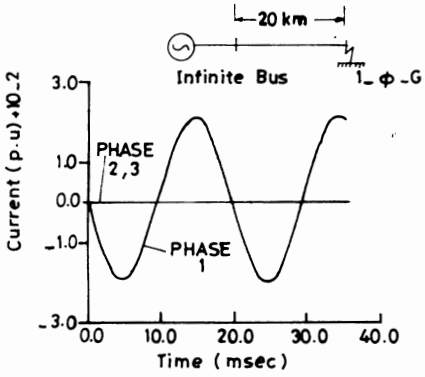

FIG. 4(a). Transient fault current waveforms.

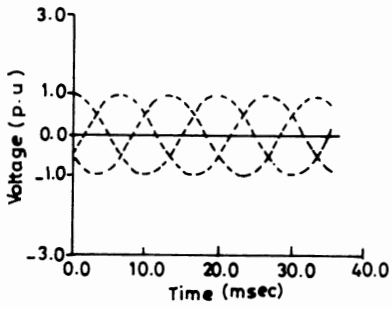

FIG. 4(b). Voltage waveforms at source end.

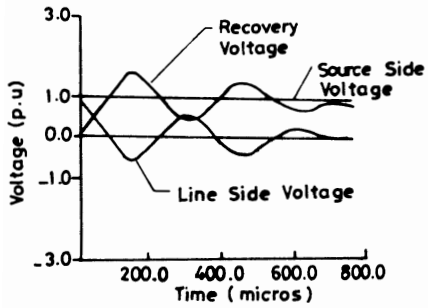

FIG. 4(c). Source-side, line-side and breaker recovery transient waveforms.

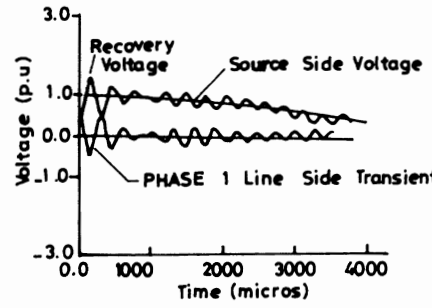

FIG. 4(d). Transient waveforms for longer observation time.

terest to note that both line-side and recovery transients are heavily damped at around 800 μsec following circuit clearance. This may be attributed to modal interaction, especially that to a greater influence of the earth mode.

4.2 Finite Source of 20000 MVA Short-Circuit Capacity

With the above finite source feeding the transmission line, Fig. 5(a) and 5(b) show current and voltage waveforms for a $1 - \phi - G$ fault at the remote end of the line. Clearly the faulted phase voltage is significantly reduced compared with the sound phase voltage. This is due to the effective source inductance and the flow of fault current in that element. Both sound phase waveforms are influenced by high frequency oscillations as aerial and earth modes propagate up and down the line. Figure 6 shows line-side source-side and recovery voltage across breaker terminals over an observation period of 800 μsec following contact separation. The influence of the source capacity is clearly demonstrated in the figure. Due to finite source effects both the peak and rate of rise of the recovery transient are markedly reduced giving better prospects of arc extinction and hence successful circuit interruption.

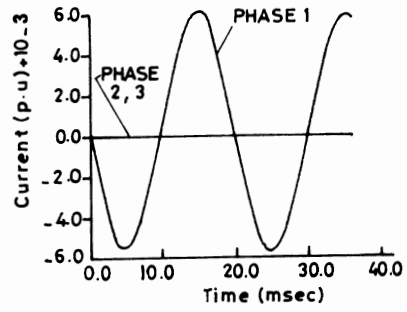

FIG. 5(a). Current waveform for finite source.

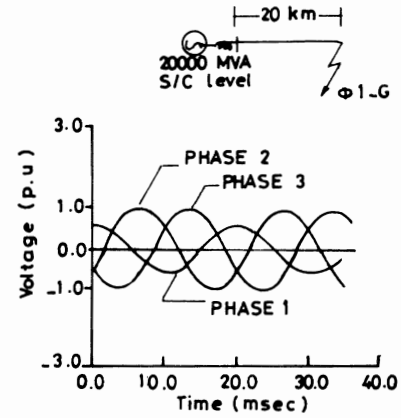

FIG. 5(b). Voltage waveform for finite source.

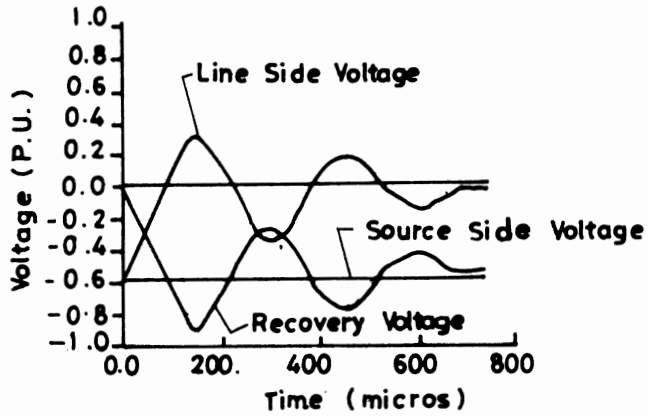

FIG. 6. Source-side, line-side and recovery waveforms.

4.3 Infinite Bus Source with 2000 pF Terminal Capacitance

The effect of bus capacitance due to terminal equipment at the source end is shown in Fig. 7(a) and Fig. 7(b) for current and voltage waveforms of $1 - \phi - G$ fault at the far end of the line. Figure 7(c) shows the results of transient voltages due to circuit interruption. Here the effect of terminal capacitance is quite noticeable on the first peak of the recovery voltage as well as its initial rate of rise. Both parameters are adversely altered and this may be alarming for enhancing circuit interruption.

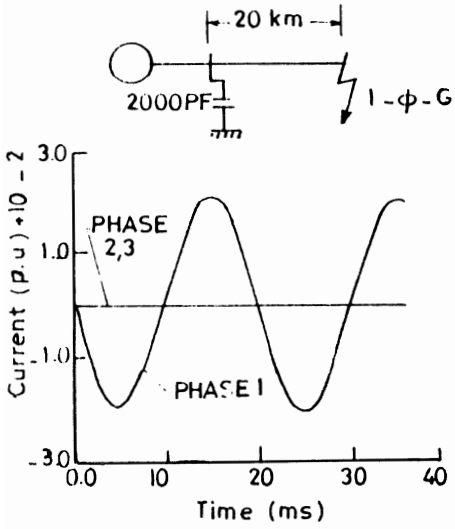

FIG. 7(a). Current waveform.

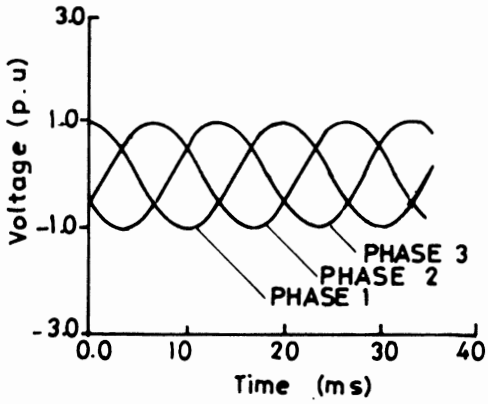

FIG. 7(b). Voltage waveform.

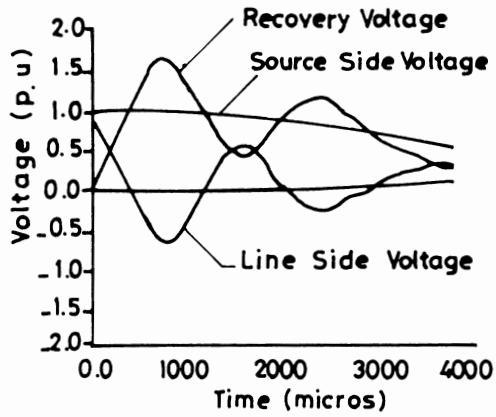

FIG. 7(c). Source-side, line-side and recovery waveforms.

5. Conclusion

The paper has presented an accurate analytical technique for the evaluation of interruption phenomena on three-phase multiconductor transmission systems. The technique is based on the theory of natural mode and Fourier Transform method and discusses the principles of simulation of fault inception as well as those of circuit interruption.

The paper has resolved two main problems. One is related to the development of a fairly accurate Fourier Transform algorithm for obtaining the wavefront of the fault current to be interrupted. The algorithm has been applied in the paper for circuit interruption around a zero cross over point of fault current. The model is also valid, however, for current chopping. The second problem is related to simulation of the effect of the circuit on the source side of the circuit breaker. An algorithm for Fourier Transform of the source side transient voltage in the existence of source inductance and terminal capacitance is developed. This transform enhances the inclusion of the source side transient component needed for the accurate analysis of interruption phenomena. The computational results presented demonstrate the validity of the models proposed for the analysis of circuit interruption in three-phase transmission systems.

References

[1] **Greenwood, A.** and **Glinkowski, M.,** Voltage escalation in vacuum switching operations. *IEEE Transactions on Power Delivery*, **3**(4) Oct., pp. 1698-1706 (1988).

[2] **Domel, H.W.,** Nonlinear and time-varying elements in digital simulation of electromagnetic transients, *IEEE Transactions of Power Apparatus and Systems*, Nov./Dec. 1971, PAS **90**(6): 2561-2567.

[3] **Phaniraj, V.** and **Phidke, A.,** Modelling of circuit breakers in the electromagnetic transients program, *IEEE Transactions on Power Apparatus and Systems*, **3**(2) May: 799-804 (1988).

[4] **Marti, J.R.,** Accurate modelling of frequency-dependent transmission lines in electromagnetic transient simulations, *IEEE Trans. PAS*, **PAS 101**(1): 147-157 (1982).

[5] **Marji, J.R.** and **Jiming, L.,** Suppression of numerical oscillations in the EMTP, *IEEE Trans. PAS,* **4**(2) May: 739-747 (1989).

[6] **Bickfor, D.J.P.** and **Abdel Rahman, M.H.,** Application of travelling-wave methods to the calculation of transient fault currents and voltages in power-system networks, *IEEE Proc., Gen. Trans. Distri,* **127-C:** 153-168 (1980).

[7] **Wedepohl, L.M.,** Application of matrix methods to the solution of travelling-wave phenomena in polyphase systems, *Proc. IEE,* **110**(12) December: 2200-2212 (1963).

[8] ———— and **Mohamed, S.E.T.,** Multiconductor transient line; theory of natural mode and Fourier integral applied to transient analysis, *Proc. IEE,* **116**(9): 1553-1563 (1969).

[9] ———— and ————, Transient analysis of multiconductor lines with special reference to nonlinear problems, *Proc. IEE,* **117**(5): 979-988 (1970).

[10] **Mullineux, N., Days, S.J.** and **Reed, J.R.,** Developments in obtaining transient response using Fourier transforms, *Int. J. Elec. Eng. Educ.,* Part I, **3:** 501-506, Part II, **4**: 31-40 (1966).

[11] **Battison, M.J., Day, S.J., Mullineux, N., Parton, K.C.** and **Reed, J.R.,** Calculation on switching phenomena in power systems, *Proc. IEE,* **114**(4): 478-486 (1967).

[12] **Langhammer, G.,** Overvoltages caused by the interruption of small inductive transformer currents, *IEEE Trans. PAS,* **3** (Aug.): 1369-1377 (1988).

[13] **Colclaser, Jr., Beeler, J.E.** and **Garrity, T.F.,** A field study of bus-fault transient recovery voltages, *IEEE Transactions on PAS,* **PAS-95**(6): 1769-1776 (1976).

[14] **St-Jean, G., Landry, M., Leclerc, M., Chénier, A.,** A new concept in past arc analysis applied to power circuit breaker, *IEEE Trans. on Power Delivery,* **3**(3) July: 1036-1044 (1988).

[15] **Van der Sluis, L.** and **Van der Linden, W.A.,** A three phase synthetic test-circuit for metal enclosed circuit breaker, *IEEE Trans on Power Delivery,* **2**(3) July: 765-771 (1987).

[16] **Bolton, E., Battisson, M.J., Bickford, J.P., Dwek, M.G., Jackson, R.L.** and **Scott, M.,** Short-line fault tests on the CEGB 275 kV system, *Proc. IEE,* **117**(4): 771 (1970).

[17] **Van der Sluis, L.** and **Janssen, A.L.J.,** Clearing faults near shunt capacitor banks, *IEEE Trans on Power Delivery,* Vol. **5**(3) July: 1346 (1990).

[18] **Engelman, N., Schreurs, E.** and **Drugge, B.,** Field test results for a multi-short 12.47 kV fault current limiter, *IEEE Trans on Power Delivery,* **6**(3) July: 1081 (1991).

Appendix I

Flow Chart of the Computer Program

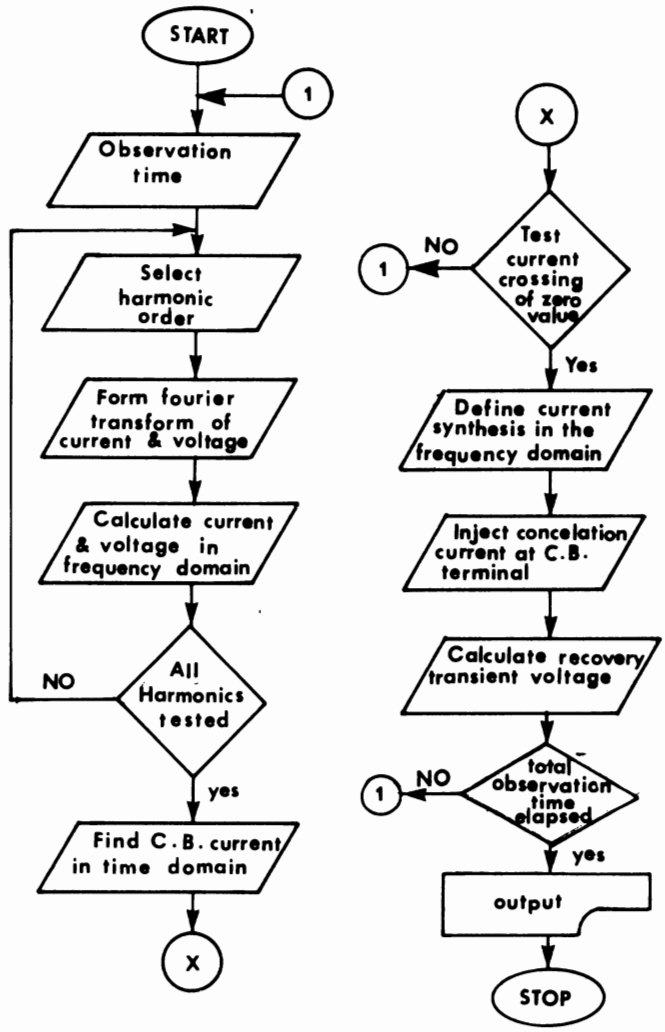

Appendix II

Line Data

Single circuit with vertical configuration

Phase conductors	= 3;	d = 30.92 cm
Earth wire	= 1;	d = 1.80 cm
Sub-bundle	= 4	
Conductor resistivity	= 32.1×10^{-9} ohm-m.	
Inductance correction factor	= 0.21088 for both phase and earth wire	
Line length	= 20 km	
Earth resistivity	= 100 ohm-m.	

ظاهـــرة القـطـــع في النـــظم الثـلاثيـــة الأطـــوار لخطـــوط النقـــل متعـــددة الموصـــلات

سليمان الطيب محمد ، و عبد العزيز عثمان محمد و أنور حسن مفتي
قسم الهندسة الكهربائية وهندسة الحاسبات ، كلية الهندسة ، جامعة الملك عبد العزيز
جـــــدة - المملكة العربية السعودية

المستخلص . مع تزايد الطلب على استخدام نظم نقل الطاقة الكهربائية ذات مستويات الفولطية المرتفعة وفائقة الارتفاع ، وما يتبع ذلك من ارتفاع في تكاليف العزل الكهربائي في مثل هذه الشبكات وأجهزتها ، تحتَمَ البحث عن وسائل لتحليل نظم القدرة للوصول إلى أقصى حدٍ ممكن في جودة التصميم . وهذا الورقة توضح أهمية وجود طريقة تحليل لنظم القدرة خلال حدوث ظاهرة القطع في النظم الثلاثية الأطوار ذات خطوط النقل المتعددة الموصلات ، كمتطلب أساسي لجودة التصميم ولتحديد دقة أجهزة القطع الكهربائية . ولقد تم تطوير طريقة رياضية في هذه الورقة لمحاكاة صدر الموجة العابرة الناتجة عن تيار الخلل ، حال بدء ظهوره ، ومن ثم استخدمت هذه الطريقة المستحدثة لحساب أمواج الفولطية المستعادة في القاطعة الكهربائية خلال الأجزاء الدقيقة من الثانية عند تباعد أقطاب القاطعة الكهربائية . وفي هذه الورقة أيضًا أخذ في الاعتبار قيم الدائرة المتغيرة على هيئة موزعة ، كما اعتبر كذلك أثر تغير الذبذبة على قيم الدائرة . وإضافة إلى ذلك ، فقد تم إيضاح أثر دائرة المنبع على معدل الارتفاع الأولي لأمواج الاستعادة وأثره على حدود قيمها العظمى .